

LA-4475

6.1

**LOS ALAMOS SCIENTIFIC LABORATORY**  
of the  
**University of California**  
LOS ALAMOS • NEW MEXICO



An Empirical Model of  
Heterogeneous Shock Initiation  
of the Explosive 9404

**For Reference**

Not to be taken from this room

UNITED STATES  
ATOMIC ENERGY COMMISSION  
CONTRACT W-7405-ENG. 36

## LEGAL NOTICE

This report was prepared as an account of work sponsored by the United States Government. Neither the United States nor the United States Atomic Energy Commission, nor any of their employees, nor any of their contractors, subcontractors, or their employees, makes any warranty, express or implied, or assumes any legal liability or responsibility for the accuracy, completeness or usefulness of any information, apparatus, product or process disclosed, or represents that its use would not infringe privately owned rights.

This report expresses the opinions of the author or authors and does not necessarily reflect the opinions or views of the Los Alamos Scientific Laboratory.

Printed in the United States of America. Available from  
Clearinghouse for Federal Scientific and Technical Information  
National Bureau of Standards, U. S. Department of Commerce  
Springfield, Virginia 22151

Price: Printed Copy \$3.00; Microfiche \$0.65

Written: July 1970  
Distributed: October 1970

LA-4475  
UC-34, PHYSICS  
TID-4500

**LOS ALAMOS SCIENTIFIC LABORATORY**  
of the  
**University of California**  
LOS ALAMOS • NEW MEXICO



An Empirical Model of  
Heterogeneous Shock Initiation  
of the Explosive 9404

by

Charles L. Mader



AN EMPIRICAL MODEL OF HETEROGENEOUS SHOCK  
INITIATION OF THE EXPLOSIVE  $\text{C}_4\text{O}_4$

by  
Charles L. Mader

ABSTRACT

An empirical model that permits numerical reproduction of the gross features of the shock initiation of the heterogeneous explosive  $\text{C}_4\text{O}_4$  in a one-dimensional hydrodynamic code is described. The model is calibrated using available experimental data.

INTRODUCTION

The objective of this study was to empirically reproduce, using a one-dimensional hydrodynamic model, the gross features of shock initiation of the heterogeneous explosive  $\text{C}_4\text{O}_4$ .

A heterogeneous explosive is one that has voids or density discontinuities that cause irregularities of the mass flow when shocked. The heterogeneous explosive is initiated by the local hot spots formed in it by shock interactions with density discontinuities. When a shock wave interacts with the density discontinuities, producing numerous local hot spots that explode but do not propagate, energy is released which strengthens the shock so that, when it interacts with additional inhomogeneities, higher-temperature hot spots are formed and more of the explosive is decomposed. The shock wave grows stronger and stronger, releasing more and more energy, until it becomes strong enough to produce propagating detonation. Most explosives of practical interest are heterogeneous.

The heterogeneous shock initiation model was first clearly confirmed experimentally by Campbell, Davis, Ramsay, and Travis.<sup>1</sup> The basic two-dimensional processes involved in the shock initiation of heterogeneous explosives have been numerically described.<sup>2-6</sup> The resulting model is called the two-dimensional hydrodynamic hot spot. The remaining numerical problem is to study the interaction

of a shock with a three-dimensional matrix of holes. The numerical solution of this problem must await development of computers several orders of magnitude faster and larger than those available in the late sixties.

The engineering requirement is for a model that will numerically reproduce the experimentally observed shock initiation behavior of explosives in a one-dimensional numerical hydrodynamic code. A one-dimensional homogeneous model cannot be satisfactory, as is discussed in Ref. 3.

One can introduce the multidimensional behavior of the flow into a hydrodynamic calculation. The behavior of the shock front can be closely approximated by the Heterogeneous-Sharp-Shock-Partial-Reaction-Burn (HSSPRB) model.

The behavior behind the shock front has been studied for over 10 years. As described in Ref. 3, Marshall (then Gittings), Craig, and Campbell in the early 1960's studied the contribution of shocked, but not detonating,  $\text{C}_4\text{O}_4$  to the velocity of metal plates. It was apparent at that time that considerable decomposition of  $\text{C}_4\text{O}_4$  occurred, releasing energy that was available to push plates. The first experimentalists to report observations of the nature of this decomposition were Dremin and Koldunov.<sup>7</sup> Using electromagnetic techniques to study the particle velocities as a function of time, they observed that the particle velocity increased with time behind, as

well as at, the shock front and observed velocity humps that moved so slowly that they did not catch up with the shock front until after complete decomposition had occurred there. We call this process "Dremin burn."

Recent studies of the Dremin burn process by Craig and Marshall<sup>8</sup> and by Kennedy<sup>9</sup> have provided a more detailed description of the process in  $\text{g}404$ . They have observed that  $\text{g}404$  shocked to low pressures ( $\sim 30$  kbar), and too thin to result in propagating detonation, does not decompose appreciably until about half a microsecond after the shock has passed through the explosive. The decomposition of the last half centimeter of explosive before the distance to detonation is reached proceeds rapidly after the initial delay. The rest of the explosive decomposes more slowly. Such complicated behavior is difficult to reproduce numerically with any of the usual pressure- or temperature-dependent decomposition expressions.

We have tried to approximate the observed Dremin burn behavior behind the shock front with an empirical, zero-order, decomposition rate law with the decomposition rate being space-dependent upon the initial distance to propagating detonation and the burn being permitted to occur only after empirically introduced time delays. The resulting model is a typical example of brute-force numerical engineering.

Properly calibrated, the HSSFRB and the Dremin burn models can be used to reproduce in a one-dimensional numerical hydrodynamic code the gross features of the heterogeneous shock initiation of the explosive  $\text{g}404$  for several interesting cases. Properly recalibrated, the model is expected to be useful for describing the shock initiation behavior of other heterogeneous explosives.

#### THE MODELS

The "experimental" heterogeneous shock initiation of  $\text{g}404$  was described in Ref. 3. The HOM equation of state<sup>2,10</sup> was used to calculate the Hugoniot for partially reacted  $\text{g}404$  using the equation-of-state parameters given in Table I. Ramsay's<sup>11</sup> unreacted equation of state,  $U_s = 0.2423 + 1.883 U_p$  (where  $U_s$  is shock velocity and  $U_p$  is particle velocity in cm/ $\mu$ sec), was used to describe the unreacted  $\text{g}404$ , and the BKW equation of state<sup>12</sup> was used to describe the  $\text{g}404$  detonation products.

The computed partially reacted HOM Hugoniot and Ramsay's experimental reactive Hugoniot,  $U_s =$

TABLE I

$\text{g}404$  HOM Equation-of-State and Input Parameters

C	+2.42300000000E-01	K	-1.61913041133E+00
S	+1.88300000000E+00	L	+5.21518534192E-01
F <sub>a</sub>	-9.04187222042E+00	M	+6.77506594107E-02
G <sub>s</sub>	-7.13185252435E+01	N	+4.26524264691E-03
H <sub>s</sub>	-1.25204979360E+02	O	+1.0467999902E-04
I <sub>a</sub>	-9.20424177603E+01	Q	+7.36422919790E+00
J <sub>s</sub>	-2.21893825727E+01	R	-4.93658222389E-01
Y <sub>s</sub>	+6.75000000000E-01	S	+2.92353060961E-02
C <sub>v</sub>	+4.00000000000E-01	T	+3.30277402219E-02
V <sub>o</sub>	+5.42299349241E-01	U	-1.14532498206E-02
$\alpha$	+5.00000000000E-05	C' <sub>v</sub>	+5.00000000000E-01
Y <sub>o</sub>	+1.20000000000E-02	Z	+1.00000000000E-01
$\mu$	+4.78000000000E-02	C <sub>R</sub>	+2.46000000000E-01
PLAP	+5.00000000000E-02	S <sub>R</sub>	+2.53000000000E+00
A	-3.53906259964E+00	PPA	-5.49963700000E+00
B	-2.57737590393E+00	PPB	-1.56863900000E+00
C	+2.60075423332E-01	D <sub>CJ</sub>	+8.88000000000E-01
D	+1.39083578508E-02	U <sub>pCJ</sub>	+2.21550000000E-01
E	-1.13963024075E-02		

Aluminum, Plexiglas, and Brass Input Parameters

	<u>Aluminum</u>	<u>Plexiglas</u>	<u>Brass</u>
$\rho_0$	2.785	1.18	8.413
C	0.535	0.2432	0.3726
S	1.35	1.5785	1.454
$\gamma$	1.70	1.0	1.87
C <sub>v</sub>	0.22	0.35	0.09
$\alpha$	$2.4 \times 10^{-5}$	$1.0 \times 10^{-4}$	$2.053 \times 10^{-5}$
Spall A	0.0714		
USP	0.250		
Y <sub>o</sub>	0.0055		
$\mu$	0.23		
PLAP	0.050		

The symbols used for the input parameters are identical to those of Ref. 10.

$0.246 + 2.53 U_p$ , are shown in Fig. 1. For each state point on the experimental reactive Hugoniot, there is a corresponding state point on a partially reacted HOM Hugoniot for some degree of reaction.

The "Pop" plot<sup>3,13</sup> for  $\text{g}404$  is an observed relationship between the initial experimental reactive Hugoniot pressure, P, and the observed distance of run to propagating detonation, X. The Pop plot for  $\text{g}404$  is shown in Fig. 2 and may be expressed by

$$\ln X = -5.499637 - 1.568639 \ln P,$$

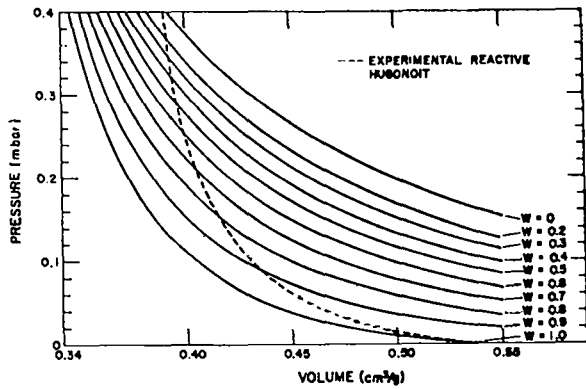


Fig. 1. The HOM 9404 partially reacted Hugoniot and the experimental reactive Hugoniot used in the HSSPRB model.

where X is in centimeters and P is in megabars.

The similarity among overlapping portions of the experimentally measured shock distance and time coordinates from experiments having different shock pressures observed by Lindstrom<sup>14</sup> for RDX/Exon and by Craig<sup>15</sup> for 9404, TNT, and TATB supports our assumption in Ref. 3 that the explosive will pass through the same P, X, and mass fraction (W) state points at the shock front regardless of the initial conditions. If this is true, we can describe the shock initiation of 9404 from the Pop plot and the experimental partially reacted Hugoniot. The resulting "experimental" description of heterogeneous shock initiation of 9404 is shown in Figs. 1 through 4.

As discussed in Ref. 3, it was not possible to reproduce the experimentally observed flow using a one-dimensional homogeneous burn model. The multi-dimensional behavior of the flow can be empirically introduced into a one-dimensional hydrodynamic calculation using the HSSPRB model described in the

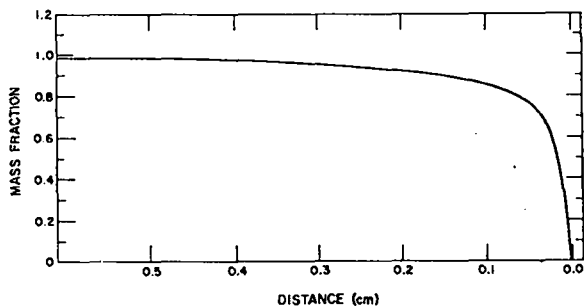


Fig. 3. The mass fraction of undecomposed 9404 explosive as a function of distance from the HSSPRB model.

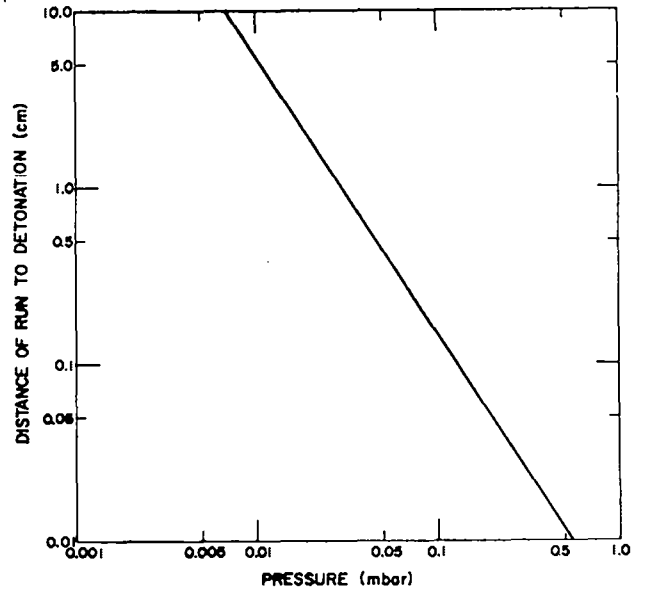


Fig. 2. The "Pop" plot for 9404.

Appendix. The HSSPRB model as used in the SIN code<sup>10</sup> reproduces the front shock behavior shown in Figs. 1 through 4. It will not reproduce the Plexiglas free-surface velocities for Plexiglas plates driven by shocked, but not detonating, 9404 observed by Craig and Marshall.<sup>8</sup> The additional energy received by the Plexiglas plates requires the introduction of an additional burn mechanism. We can approximate the observed Plexiglas free-surface velocities if the empirical, zero-order, Dremin burn rate law,

$$\frac{dw}{dt} = -K_D(w),$$

is introduced into the calculation; if the Dremin

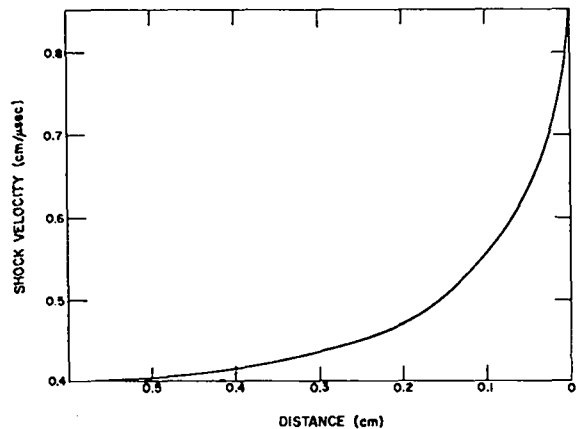


Fig. 4. The shock velocity of the front of the reactive shock in 9404 from the HSSPRB model.

burn constant,  $K_D$ , is a function of the initial distance of run to propagating detonation,  $X$ ,

$$K_D = 0.2247 - 0.0449(X) ,$$

$$K_D = 2.0 \text{ if } X < 0.55 ,$$

$$K_D = 0.0 \text{ if } X > 5.0 ;$$

and if the burn is started from 0.1 to 0.5  $\mu\text{sec}$  after the shock arrives at an  $X$  of 0.55 or at an inert interface. The constants given are the result of attempting to numerically reproduce the available experimental data on  $\text{9404}$  being shocked at between 10 and 63 kbar and at distances to detonation ( $X$ ) of 5 to 0.33 cm. Individual experiments can be better reproduced if the parameters are calibrated to each of them. It is necessary to change the time at which to start the burn for the various systems studied, apparently depending upon whether the explosive receives a shock or a rarefaction during the interval before appreciable Dremin burn occurs.

Figure 5 shows the calculated pressure-distance and mass-fraction-distance profiles for  $\text{9404}$  initially shocked to 50 kbar with the HSSPRB model alone, and Fig. 6 shows the calculated profiles with Dremin burn included. Figure 7 shows the calculated and experimental free-surface velocity of a 0.2-cm-thick Plexiglas plate in contact with 0.250 and 0.630 cm of  $\text{9404}$  shocked to 30 kbar by an explosive system consisting of 1.092 cm of Plexiglas, 1.143 cm of steel, 1.778 cm of polyethylene, 2.54 cm of Baratol, and a P-80 lens. The calculations were performed with the Plexiglas singly shocked to 0.022 mbar and a particle velocity of 0.0565 cm/ $\mu\text{sec}$ . The calculated distance of run to detonation was 1.0 cm. The smoothed experimental data of Craig and Marshall are also shown. The time to Dremin burn the 0.63-cm-thick piece was taken as 0.55  $\mu\text{sec}$  after the shock arrived at the  $X = 0.55$  cm to detonation position. The time to Dremin burn of the 0.25-cm-thick piece was taken as 0.20  $\mu\text{sec}$  after the shock arrived at the second explosive-Plexiglas interface. Figure 8 shows the calculated pressure-distance and mass fraction-distance profiles for 0.630-cm-thick  $\text{9404}$  shocked to 30 kbar. Figure 9 shows the calculated and experimental free-surface velocity of a 0.5-cm-thick Plexiglas plate in contact with 0.25 cm of  $\text{9404}$  shocked to 63 kbar

by an explosive system consisting of 1.27 cm of Dural, 1.27 cm of brasa, 5.08 cm of Boracitol, and a P-120 lens. The calculations were performed with the Dural singly shocked to 0.0936 mbar and to a particle velocity of 0.05516 cm/ $\mu\text{sec}$ . The initial interface velocity was 0.075 cm/ $\mu\text{sec}$ . The calculated distance of run to detonation was 0.335 cm. The time to Dremin burn was taken as 0.2  $\mu\text{sec}$ .

Similar calculations were performed for other systems, and it was observed that if the explosive thickness exceeded that necessary for propagating detonation, the Dremin burn time required to reproduce the experimental data was shorter ( $\sim 0.1$   $\mu\text{sec}$ ) than if the explosive thickness was less than necessary for propagating detonation. Also, systems with higher initial shock pressures were better described if a short ( $\sim 0.1$ - $\mu\text{sec}$ ) Dremin burn was used. Calculations were also performed for the short-duration shocks reported by Gittings.<sup>16</sup> The rarefactions from the rear did catch up with the front before detonation occurred, but because the model will not respond to either shocks or rarefactions, except indirectly by use of the Dremin burn time, further numerical engineering will be required before failure and propagation of the detonation can be described. The Gittings data should be adequate for calibration of a model that responds to rarefactions.

#### CONCLUSIONS

An empirical model that permits numerical reproduction of some observed features of the shock initiation of the heterogeneous explosive,  $\text{9404}$ , in a one-dimensional hydrodynamic code can be described and calibrated with available experimental data.

It is reasonable to conclude that significant decomposition of the explosive occurs in the experimental geometries studied in this report. The decomposition is a result of complicated three-dimensional flow and chemical kinetics. Any empirical one-dimensional model of such a complicated three-dimensional process will have limited usefulness and will require improvements and recalibration as additional experimental data become available.

#### ACKNOWLEDGMENTS

The author gratefully acknowledges the experimental studies by Elisabeth F. Marshall, Group GMX-4 and Bobby G. Craig, Group GMX-8, which were so essential to this work. Elisabeth Marshall, B.G. Craig, and A. W. Campbell, in 1961, performed their first series

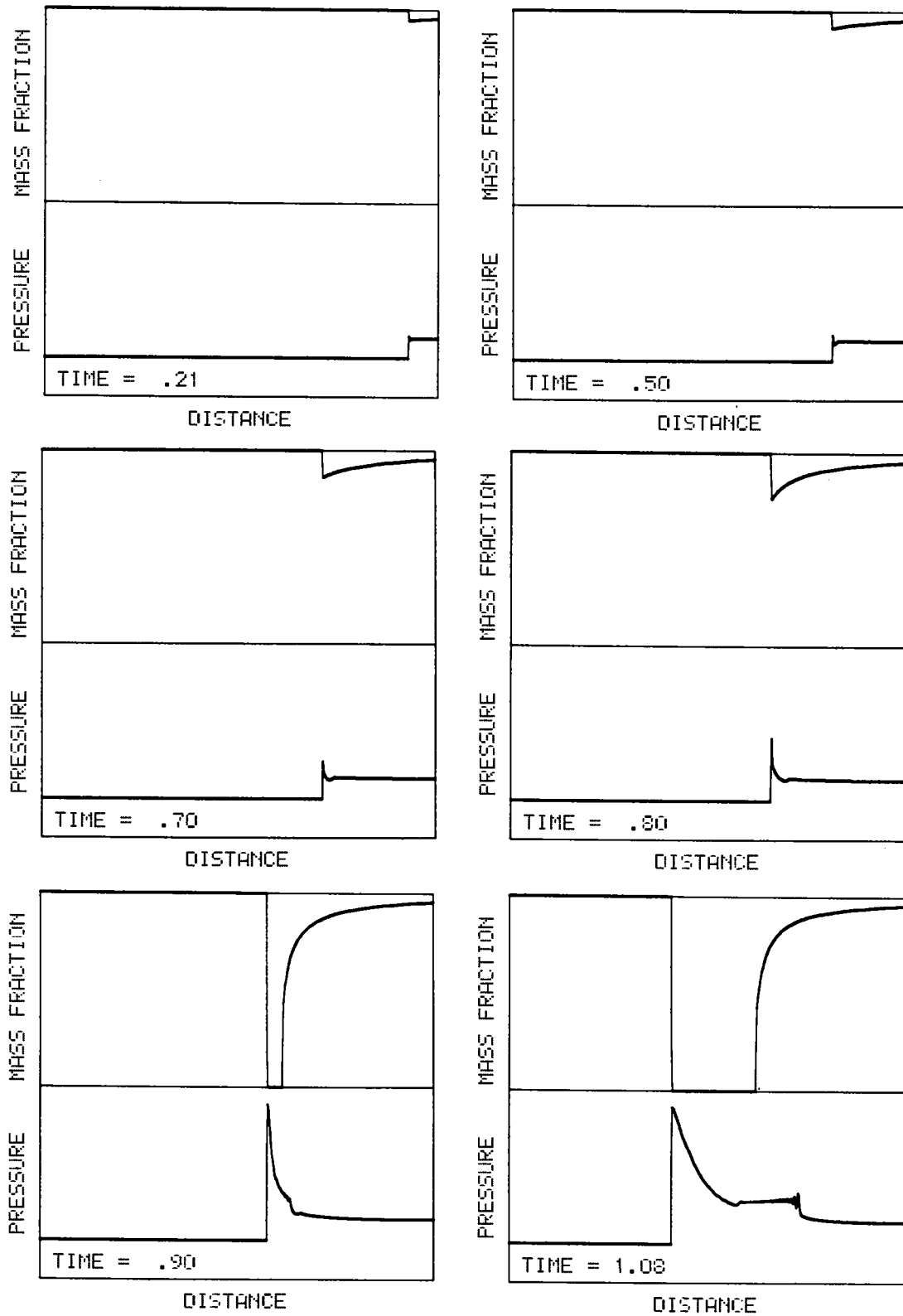


Fig. 5. The pressure-distance and mass fraction-distance profiles for 9404 calculated using the HSSPRB model alone. The 9404 was initially shocked to 50 kbar. The distance to detonation was 0.45 cm. The pressure scale is from -100 to +400 kbar, the distance scale from 0 to 1.0 cm, and the mass fraction scale from 0 to 1.0.



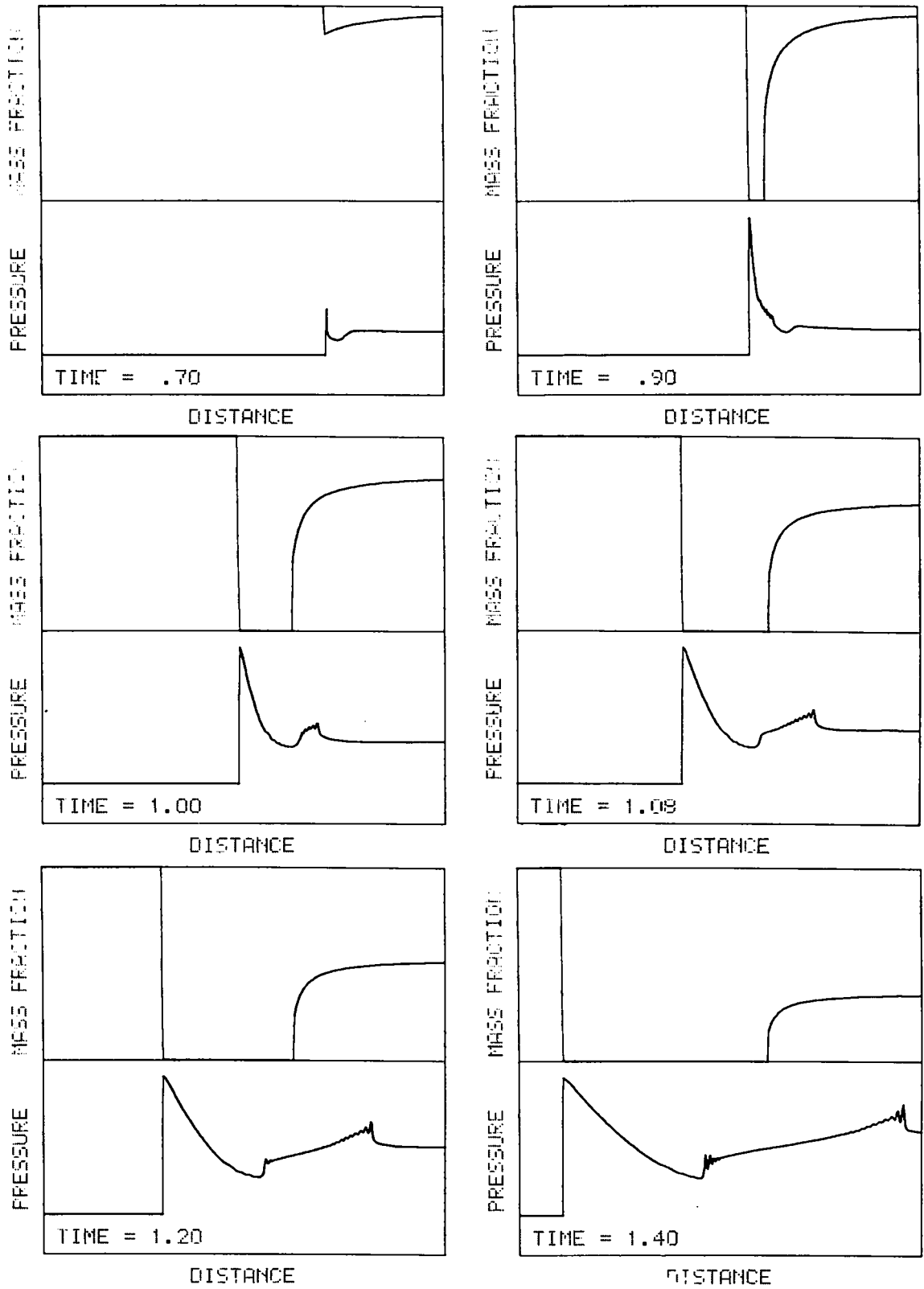


Fig. 6. The pressure-distance and mass fraction-distance profiles for 9404 calculated using the HSSPRB model with Dremis burn included. The 9404 was initially shocked to 50 kbar. The Dremis burn time was 0.2  $\mu$ sec. The scales are the same as those in Fig. 5.

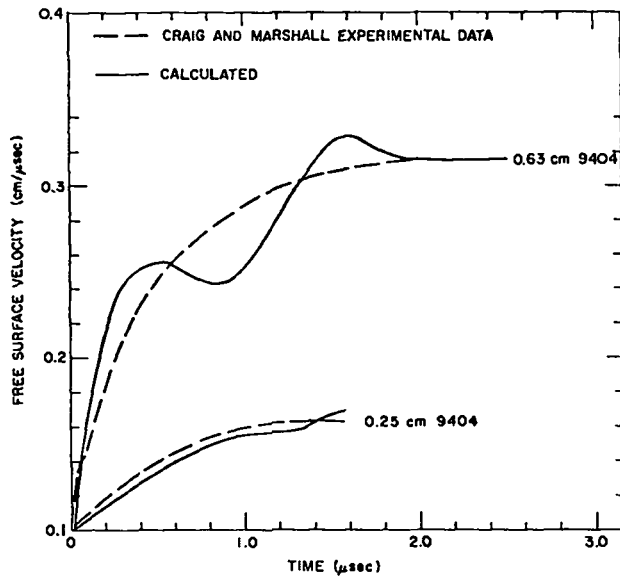


Fig. 7. The free-surface velocity of 0.20-cm-thick Plexiglas plates in contact with 0.25- and 0.63-cm-thick pieces of 9404 initially shocked to 30 kbar.

of experiments that suggested that considerable decomposition of 9404 occurred behind the shock front. A. N. Dremin of the U.S.S.R. independently observed similar behavior in pressed TNT and described his results to this author at the Twelfth Symposium on Combustion. Dremin's observations furnished the first approximate description of the nature of the flow behind the shock front.

The author also gratefully acknowledges the contributions of A. W. Campbell, William C. Davis, Bobby G. Craig, John B. Ramsay, Bernard Hayes, and James R. Travis, GMX-8; Wildon Fickett, GMX-10; S. Robert Orr and George N. White, Jr., T-5; Louis C. Smith, GMX-2; Ian Skidmore, AWRE; and O. Jones and J. E. Kennedy, Sandia Corporation.

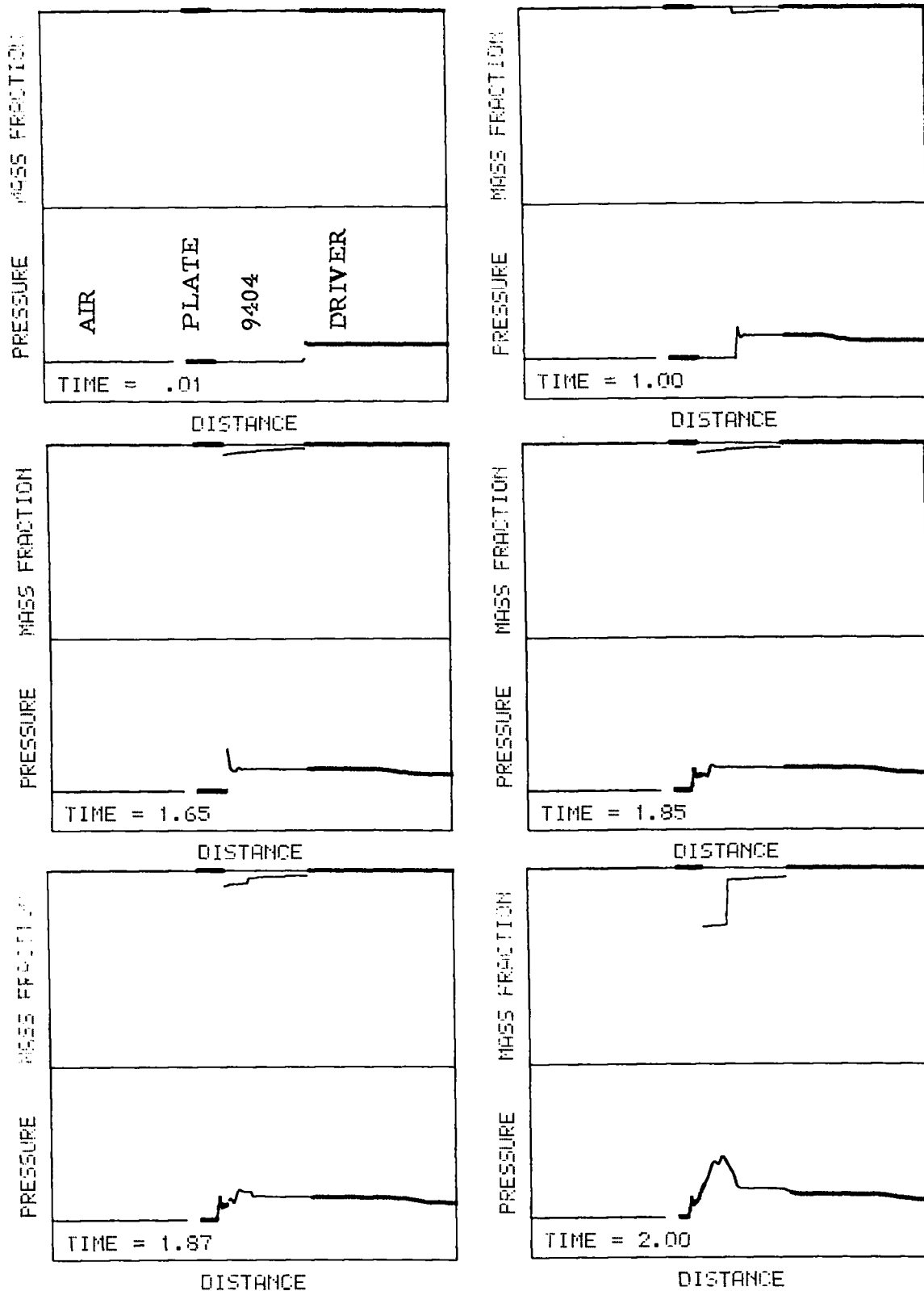


Fig. 8. The pressure-distance and mass fraction-distance profiles for the 0.63-cm thick piece of 9404 of Fig. 7. The dark points on the right are the Plexiglas driver; the light points next on the left are for the 0.63-cm 9404, followed by dark points for the 0.2-cm Plexiglas plate and then light points for air at the extreme left. The pressure scale is from -100 to +200 kbar, the distance scale from 0 to  $(2.835 - (0.0565)(\text{TIME}))$  cm, and the mass fraction scale from 0 to 1.0.

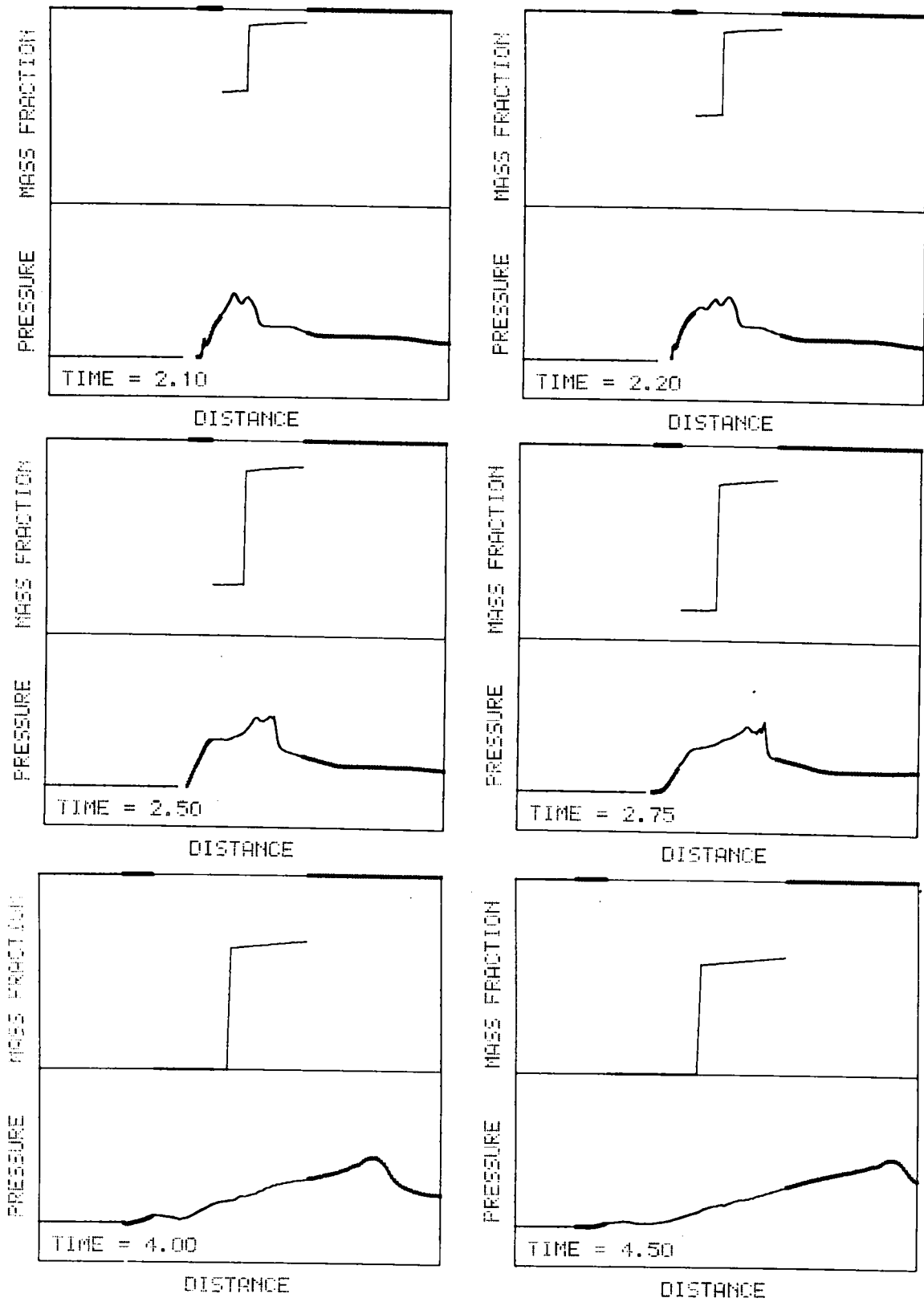


Fig. 8.(Cont.)

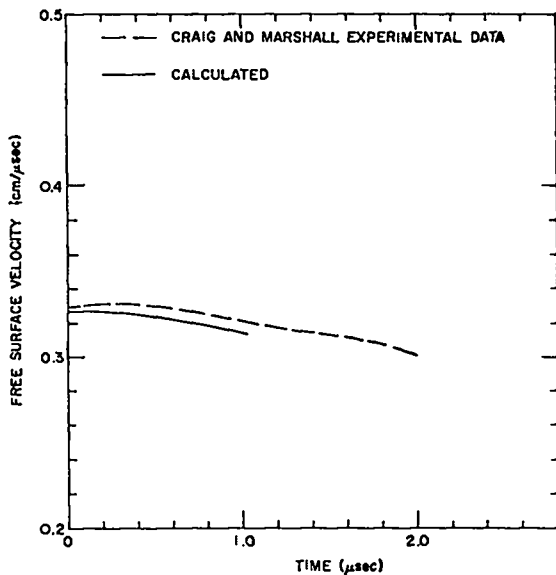


Fig. 9. The free-surface velocity of a 0.5-cm-thick Plexiglas plate in contact with 0.254 cm of  $\text{Q}+\text{O}_4$  initially shocked to 63 kbar.

#### APPENDIX

##### THE SHARP-SHOCK AND HSSPRB AND DREMIN BURN OPTIONS OF THE SIN CODE

The reader is assumed to be acquainted with the contents of the report<sup>10</sup> describing the SIN code. This appendix is intended as a supplement to LA-3720. The Sharp-Shock Burn

The sharp-shock burn option is suitable for plane and converging geometry, but not for diverging geometry.

A sharp-shock burn burns a cell of explosive after compressing it by moving the right cell boundary at C-J particle velocity for an interval of time determined by the detonation velocity.

The energy of the cell is set equal to the Hugoniot energy at the compressed density. In slab geometry, the process continues through the explosive at the input detonation velocity. For converging geometry, the increased density resulting from convergence also results in an increased pressure from which one can calculate a new detonation and particle velocity. These new velocities are used to compress the next cell.

In practice, the time steps used in the calculation are one-fourth of the time required to compress the cell to C-J density, and four time steps occur before the cell is burned. When the shock arrives at a new explosive, the new input C-J deto-

nation and particle velocities are used to compress the new explosive. This is useful for explosive systems such as a Baratol lens initiating a higher performance, slightly underdriven explosive such as Composition B. It will obviously not correctly calculate an overdriven, or significantly underdriven, detonation. The advantages of a sharp-shock burn are that one can obtain excellent Taylor waves using a small number of cells to describe multiple layers of explosives in plane or converging geometry. The disadvantages are that it requires more information and more artificial constraints than do the C-J volume or Arrhenius-burn techniques. The sharp-shock burn can give incorrect results for systems in diverging geometry (as will the C-J volume burn) and for systems that are overdriven or significantly underdriven. The sharp-shock burn as presently coded in SIN cannot handle sandwiches of explosives and inert material.

If the burn option is set equal to 3 for an explosive, the explosive is burned using the sharp-shock burn procedure. The code assumes that the explosive is burned from right to left or from large to smaller  $j$  ( $j$  = net point of Lagrangian mesh). The explosive with the largest  $j$  is assumed to be a right-boundary piston, with the initial velocity being the C-J particle velocity and the final velocity being the lowest particle velocity permitted. Multiple explosive slabs may be calculated if the explosives are not overdriven. The burn option of 3 assumes that the 11th component card contains the C-J detonation velocity in columns 55 through 72 and, if the explosive is not that with the largest  $j$ , the C-J particle velocity in columns 37 through 54. The sharp-shock burn has been coded into the SIN code as follows.

SSBC - Used to count the number of time steps. If equal to 4, the current cell being compressed is burned.

ICF (Spall Flag) - If equal to 3, the cell is being compressed and is the next cell to be burned.

In BURN subroutine

If cell ICF does not equal 3, skip burn subroutine  
If cell ICF equals 3, then

- a. If SSBC < 4, set CP (cell pressure) =  $P_0$
- b. If SSBC = 4, set CP equal to HOM Hugoniot pressure for cell volume CV, set CI equal

to HOM Hugoniot energy for cell volume, and set CW equal to zero.

The ICF = 3 flag is moved to the next cell unless the next cell IERN does not equal 3; then, SSBC is set equal to zero, the sharp-shock burn option is void, and the viscosity constant is set equal to 2.0.

The new detonation velocity,  $D_{CJ}$ ; particle velocity,  $U_{CJ}$ ; and time step,  $\Delta t$ , are calculated from

$$D_{CJ} = V_o [P_{CJ} / (V_o - V_{CJ})]^{0.5},$$

$$U_{CJ} = [P_{CJ} (V_o - V_{CJ})]^{0.5},$$

$$\Delta t = (\Delta X / D_{CJ}) 0.25,$$

where

$$P_{CJ} = CP, V_{CJ} = CV \text{ of cell just burned.}$$

In the general FSIN control routine

1. The CU (cell particle velocity) is set equal to  $-U_{CJ}$  for front cell right boundary if slab geometry ( $\alpha = 1$ ).  
If  $\alpha > 1$  (cylindrical or spherical geometry), the above method is used for the first 49 cycles. Then  $CU_{j+1} = CU_{j+2}$  where  $j+1$  is front cell right boundary and  $j+2$  is next boundary behind  $j+1$ .
2. The CI (cell energy) is not calculated for the two cells next to the front.
3. The CP (cell pressure) is not calculated for the cell next to the front.
4. The other variables are calculated only to the cell at the front.
5. The viscosity constant is set equal to 0.01 until all the explosive is burned. Then it is set equal to 2.0 (in Burn routine).
6. When the detonation wave arrives at the interface between explosives, the cell particle and detonation velocity are set equal to input values.

#### The HOM Equation of State

If IND = 3, calculates Hugoniot pressure and energy for input V. Iterates six times on  $I_H = \frac{1}{2} P(V_o - V)$  and  $P = P_I + \frac{1}{\beta V} (I_H - I_I)$  with  $P = P_I$  initially.

#### The Heterogeneous Sharp-Shock Partial Reaction Burn and the Dremin Burn

If the burn option is set equal to 4 for an explosive, it is burned using the following HSSPRB and Dremin-burn procedure. The features of the sharp-shock burn are used with the additional feature that the shock front is forced to assume the behavior prescribed by the experimentally calibrated, single-curve, heterogeneous initiation model. Given the initial explosive interface velocity,  $U_p$ , the distance to full-order detonation is calculated using the reactive Hugoniot  $C_R$  and  $S_R$  to calculate the shock velocity,  $U_s$ .

$$U_s = C_R + S_R(U_p),$$

from which the pressure on the reactive Hugoniot,  $P_R$ , can be calculated using

$$P_R = \frac{U_s^2 - (U_s)(C_R)}{(S_R)(V_o)}.$$

The distance to detonation, X, is then calculated from the Pop plot

$$\ln X = PPA + (FPB)(\log P_R).$$

The time step is calculated from

$$\Delta t = \left(\frac{\Delta X}{U_s}\right) 0.25.$$

The cell is compressed for four time cycles using the initial explosive interface velocity,  $U_p$ .

Given the specific volume, V, of the compressed cell, we can calculate the reactive Hugoniot pressure and energy of the cell from

$$P_R = \frac{C_R^2 (V_o - V)}{[V_o - S_R (V_o - V)]^2},$$

$$I_R = \frac{1}{2} (P_R) (V_o - V).$$

The only remaining unknown state value is the amount of reaction of cell W (mass fraction of undecomposed explosive) associated with the particular partially reacted Hugoniot that has state points  $P_R$ ,  $I_R$ , and V. We iterate, using linear feedback, on W

until the HOM pressure is within  $5 \times 10^{-4}$  of  $P_R$ . The cell is then "partially burned" by setting the cell  $W$  and energy to the values just calculated.

We then reduce the distance to detonation by  $\Delta X$ , and calculate a new  $P_R$  from the Pop plot equation, a new shock velocity, a particle velocity, and a time step. The new (higher) particle velocity is applied for four time cycles, giving us a new cell volume, and the calculation is continued as described above. This procedure is continued until the cell particle velocity is equal to the input C-J velocity, at which time the burn option is set equal to 3 and the burning is continued as a sharp-shock burn. The HSSPRB technique just described will reproduce the experimentally observed behavior of the shock front initiating a heterogeneous explosive.

The Dremin burn model is included to try to describe the behavior behind the shock front. When the cell is burned, the distance to propagating detonation  $X$  is used to calculate the Dremin burn constant,  $K_D$ , using

$$K_D = DCA + DCB(X) .$$

$$\text{If } X < DEX, K_D = HDEC .$$

$$\text{If } X > 5.0, K_D = 0.0 .$$

$K_D$  becomes a cell constant that is used to burn the explosive after the time, DBTIME, has expired, using

$$W_j^{n+1} = W_j^n \left[ 1.0 - (K_D)_j (\Delta t) \right] .$$

The Dremin burn time is counted from whenever any of the following options first occur:  $X < DEX$ ,  $X = 0.0$ , or an interface is reached by the shock wave. If the burn option is equal to 4, the following input is required by the SIN code.

#### 11th Component Card

Col.	Format	
1-18	E18.11	$W_0$
19-36	E18.11	PPA
37-54	E18.11	PPB
55-72	E18.11	C-J Detonation Velocity

#### 12th Component Card

1-18	E18.11	$C_R$
19-36	E18.11	$S_R$
37-54	E18.11	C-J Particle Velocity
55-72	E18.11	Initial explosive interface particle velocity to be used if explosive is not largest $j$ component. Otherwise is zero, and the initial-final piston velocity is used for the initial explosive interface particle velocity.

#### 13th Component Card

1-18	E18.11	DCA
19-36	E18.11	DCB
37-54	E18.11	DBTIME
55-72	E18.11	DEX

#### 14th Component Card

1-18	E18.11	HDEC
------	--------	------

The gas or explosive cards become cards 15 through 19.

As they presently are coded in SIN, the HSSPRB and Dremin-burn options are suitable for only a certain type of problem. The shocks are assumed to be plane and flat-topped. Additional experimental and theoretical studies will be required before the effect of reflected shocks or rarefactions on the decomposition of the explosive can be included in the model.

#### REFERENCES

1. A. W. Campbell, W. C. Davis, J. B. Ramsay, and J. R. Travis, "Shock Initiation of Solid Explosives," Phys. Fluids 4, 511 (1961).
2. Charles L. Mader, "The Two-Dimensional Hydrodynamic Hot Spot," Los Alamos Scientific Laboratory report LA-3077 (1964).
3. Charles L. Mader, "The Two-Dimensional Hydrodynamic Hot Spot, Vol. II," Los Alamos Scientific Laboratory report LA-3235 (1965).
4. Charles L. Mader, "The Two-Dimensional Hydrodynamic Hot Spot, Vol. III," Los Alamos Scientific Laboratory report LA-3450 (1966).
5. Charles L. Mader, "The Two-Dimensional Hydrodynamic Hot Spot, Vol. IV," Los Alamos Scientific Laboratory report LA-3771 (1967).

6. Charles L. Mader, "Initiation of Detonation by the Interaction of Shocks with Density Discontinuities," *Phys. Fluids* 8, 1811 (1965).
7. A. N. Dremin and S. A. Koldunov, "Initiation of Detonation by Shock Waves in Cast and Pressed TNT," *Vzryvnoe Delo*, 63, 37 (1967).
8. B. G. Craig and E. F. Marshall, "Behavior of a Heterogeneous Explosive when Shocked but not Detonated," Fifth Symposium (International) on Detonation, Pasadena, California, August 1970.
9. J. E. Kennedy, "Quartz Gauge Study of Upstream Reaction in a Shocked Explosive," Fifth Symposium (International) on Detonation, Pasadena, California, August 1970.
10. Charles L. Mader and William R. Gage, "FORTRAN SIN - A One-Dimensional Hydrodynamic Code for Problems which Include Chemical Reactions, Elastic-Plastic Flow, Spalling, and Phase Transitions," Los Alamos Scientific Laboratory report LA-3720 (1967).
11. J. B. Ramsay, private communication.
12. Charles L. Mader, "Detonation Properties of Condensed Explosives Computed Using the Becker-Kistiakowsky-Wilson Equation of State," Los Alamos Scientific Laboratory report LA-2900 (1963).
13. John B. Ramsay and A. Popolato, "Analysis of Shock Wave and Initiation Data for Solid Explosives," Fourth Symposium (International) on Detonation, White Oak, Maryland, October 1965, ACR-126, 233 (1965).
14. I. E. Lindstrom, "Plane Shock Initiation of an RDX Plastic Bonded Explosive," *J. Appl. Phys.* 37, 4873 (1966).
15. B. G. Craig, private communication.
16. Elisabeth F. Gittings, "Initiation of a Solid Explosive by a Short-Duration Shock," Fourth Symposium (International) on Detonation, White Oak, Maryland, October, 1965, ACR-126, 373 (1965).